Metallic Contact Formation for Molecular Electronics: Interactions between Vapor-Deposited Metals and Self-Assembled Monolayers of Conjugated Mono- and Dithiols

Bert de Boer,[†,§] Martin M. Frank,[‡,||] Yves J. Chabal,[‡] Weirong Jiang,[‡] Eric Garfunkel,[‡] and Zhenan Bao*[,†,⊥]

Bell Laboratories, Lucent Technologies, 600 Mountain Avenue, Murray Hill, New Jersey 07974, and Rutgers University, Department of Chemistry and Chemical Biology, Piscataway, New Jersey 08854

Received September 2, 2003. In Final Form: December 10, 2003

We present grazing-incidence Fourier transform infrared and AFM data of Au, Al, and Ti vapor-deposited onto self-assembled monolayers (SAMs) of conjugated mono- and dithiols. SAMs of 4,4‴-dimercapto-*p*-quaterphenyl, 4,4″-dimercapto-*p*-terphenyl, and 4,4′-dimercapto-*p*-biphenyl have reactive thiols at the SAM/vacuum interface that interact with vapor-deposited Au or Al atoms, preventing metal penetration. Conjugated monothiols lack such metal blocking groups, and metals (Au, Al) can penetrate into their SAMs. Vapor deposition of Ti onto conjugated mono- and dithiol SAMs and onto hexadecanethiol SAMs destroys the monolayers.

Although Aviram and Ratner proposed the concept of using a single molecule as a rectifier,[1] nearly three decades ago, serious experimental research into single molecular electronics has only begun this past decade. Most of the recent work is based on utilizing thiol-functionalized molecules on group Ib metals, because they are known to form well-ordered, densely packed self-assembled monolayers (SAMs).[2] To study the electronic properties of conjugated SAMs, metal/organic interfaces are typically formed to connect them to macroscopic metallic contacts. In this geometry, a gold substrate usually serves as the bottom electrode. As a top electrode, a conducting atomic force microscope (c-AFM) or scanning tunneling microscope (STM) tip is frequently used.[3−6] In other examples, the top electrode is prepared by vapor deposition of a metal through a mask.[7,8] While using a c-AFM or STM tip is convenient for fundamental studies of single (or few) molecules, it is difficult to fabricate arrays of devices required for electrical circuits and interconnects in this manner.[7,8] Vapor deposition of metals (e.g., Au, Ag, Cu, Al, Ti, Cr, and Fe) on alkanethiols with organic functional end groups (OFGs) such as CH_3, OH, COOH, CO_2CH_3, CN, SH, and CF_3 has been studied extensively,[9−17] but reports on vapor deposition of metals onto conjugated SAMs with OFGs are scarce.[18,19] Conjugated SAMs have been used for modification of electrodes,[20] sensors,[21] molecular switches,[22] and rectifiers.[23] Therefore, it is important to understand the effect of metal deposition on

* Corresponding author. E-mail: zbao@chemeng.stanford.edu. Tel: 650-723-2419. Fax: 650-723-9780.

† Lucent Technologies.

‡ Rutgers University.

§ Permanent address: Molecular Electronics: Physics of Organic Semiconductors, Materials Science Centre, University of Groningen, Nijenborgh 4, NL-9747AG, Groningen, The Netherlands.

|| New address: IBM T.J. Watson Research Center, Yorktown Heights, NY 10598.

⊥ New address: Department of Chemical Engineering, Stanford University, Stanford, CA 94305.

(1) Aviram, A.; Ratner, M. A. *Chem. Phys. Lett.* **1974**, *29*, 277.

(2) de Boer, B.; Meng, H.; Perepichka, D. F.; Zheng, J.; Frank, M. M.; Chabal, Y. J.; Bao, Z. *Langmuir* **2003**, *19*, 4272.

(3) (a) Cui, X. D.; Primak, A.; Zarate, X.; Tomfohr, J.; Sankey, O. F.; Moore, A. L.; Moore, T. A.; Gust, D.; Harris, G.; Lindsay, S. M. *Science* **2001**, *294*, 571. (b) Cui, X. D.; Primak, A.; Zarate, X.; Tomfohr, J.; Sankey, O. F.; Moore, A. L.; Moore, T. A.; Gust, D.; Nagahara, L. A.; Lindsay, S. M. *J. Phys. Chem.* **2002**, *106*, 8609.

(4) Fan, F. R.-F.; Yang, J.; Dirk, S. M.; Price, D. W.; Kosynkin, D.; Tour, J. M.; Bard, A. J. *J. Am. Chem. Soc.* **2001**, *123*, 2454.

(5) Rawlett, A. M.; Hopson, T. J.; Nagahara, L. A.; Tsui, R. K.; Ramachandran, G. K.; Lindsay, S. M. *Appl. Phys. Lett.* **2002**, *81*, 3043.

(6) Ng, M.-K.; Lee, D.-C.; Yu, L. *J. Am. Chem. Soc.* **2002**, *124*, 11862.

(7) (a) Collier, C. P.; Wong, E. W.; Belohradský, M.; Raymo, F. M.; Stoddart, J. F.; Keukes, P. J.; Williams, R. S.; Heath, J. R. *Science* **1999**, *285*, 391. (b) Collier, C. P.; Mattersteig, G.; Wong, E. W.; Luo, Y.; Beverly, K.; Sampaio, J.; Raymo, F. M.; Stoddart, J. F.; Heath, J. R. *Science* **2000**, *289*, 1172.

(8) (a) Chen, J.; Wang, W.; Reed, M. A.; Rawlett, A. M.; Price, D. W.; Tour, J. M. *Appl. Phys. Lett.* **2000**, *77*, 1224. (b) Chen, J.; Reed, M. A. *Chem. Phys.* **2002**, *281*, 127.

(9) Jung, D. R.; Czanderna, A. W. *Crit. Rev. Solid State Mater. Sci.* **1994**, *19*, 1.

(10) Herdt, G. C.; Jung, D. R.; Czanderna, A. W. *Prog. Surf. Sci.* **1995**, *50*, 103.

(11) Tarlov, M. J. *Langmuir* **1992**, *8*, 80.

(12) (a) Ohgi, T.; Sheng, H.-Y.; Dong, Z.-C.; Nejoh, H. *Surf. Sci.* **1999**, *442*, 277. (b) Ohgi, T.; Fujita, D.; Deng, W.; Dong, Z.-C.; Nejoh, H. *Surf. Sci.* **2001**, *493*, 453. (c) Oghi, T.; Sheng, H.-Y.; Nejoh, H. *Appl. Surf. Sci.* **1998**, *130−132*, 919. (d) Ohgi, T.; Sheng, H.-Y.; Dong, Z.-C.; Nejoh, H.; Fujita, D. *Appl. Phys. Lett.* **2001**, *79*, 2453.

(13) Fisher, G. L.; Hooper, A. E.; Opila, R. L.; Allara, D. L.; Winograd, N. *J. Phys. Chem. B* **2000**, *104*, 3267.

(14) Konstadinidis, K.; Zhang, P.; Opila, R. L.; Allara, D. L. *Surf. Sci.* **1995**, *338*, 300.

(15) Hooper, A. E.; Fisher, G. L.; Konstadinidis, K.; Jung, D.; Nguyen, H.; Opila, R. L.; Collins, R. W.; Winograd, N.; Allara, D. L. *J. Am. Chem. Soc.* **1999**, *121*, 8052.

(16) Fisher, G. L.; Walker, A. V.; Hooper, A. E.; Tighe, T. B.; Bahnck, K. B.; Skriba, H. T.; Reinard, M. D.; Haynie, B. C.; Opila, R. L.; Winograd, N.; Allara, D. L. *J. Am. Chem. Soc.* **2002**, *124*, 5528.

(17) Carlo, S. R.; Wagner, A. J.; Fairbrother, D. H. *J. Phys. Chem. B* **2000**, *104*, 6633.

(18) Haynie, B. C.; Walker, A. V.; Tighe, T. B.; Allara, D. L.; Winograd, N. *Appl. Surf. Sci.* **2003**, *203−204*, 433.

(19) Chang, S.-C.; Li, Z.; Lau, C. N.; Larade, B.; Williams, R. S. *Appl. Phys. Lett.* **2003**, *83*, 3198.

(20) (a) Dudek, S. P.; Sikes, H. D.; Chidsey, C. E. D. *J. Am. Chem. Soc.* **2001**, *123*, 8033. (b) Zhu, L. H.; Tang, H. Q.; Harima, Y.; Yamashita, K.; Hirayama, D.; Aso, Y.; Otsubo, T. *Chem. Commun.* **2001**, 1830. (c) Campbell, I. H.; Kress, J. D.; Martin, R. L.; Smith, D. L.; Barashkov, N. N.; Ferraris, J. P. *Appl. Phys. Lett.* **1997**, *71*, 3528. (d) Zehner, R. W.; Parsons, B. F.; Hsung, R. P.; Sita, R. L. *Langmuir* **1999**, *15*, 1121.

(21) Hutchison, J. E.; Postlethwaite, T. A.; Murray, R. W. *Langmuir* **1993**, *9*, 3277.

(22) Chen, J.; Reed, M. A.; Rawlett, A. M.; Tour, J. M. *Science* **1999**, *286*, 1550.

10.1021/la0356349 CCC: $27.50
Published on Web 01/27/2004

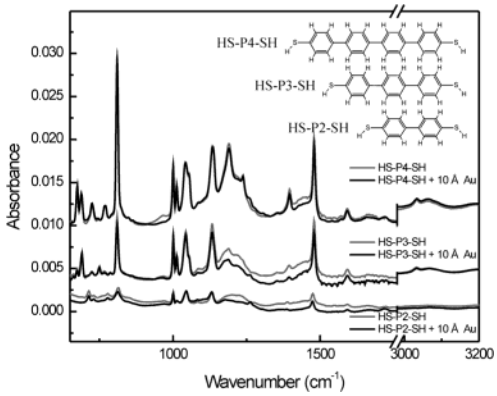

Figure 1. GI-FTIR spectra of HS-P4-SH, HS-P3-SH, and HS-P2-SH before (gray) and after (black) deposition of 10 Å Au. A vertical offset is introduced for clarity (0.003 and 0.010 units for HS-P3-SH and HS-P4-SH, respectively).

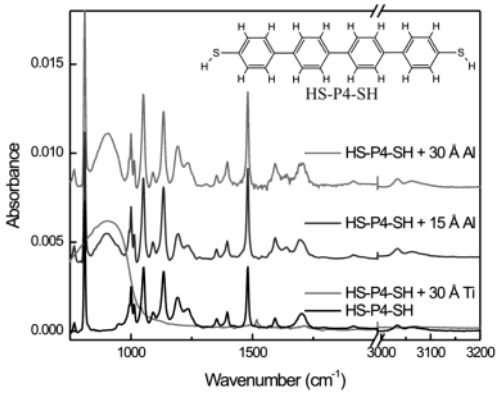

Figure 2. GI-FTIR spectra of pristine HS-P4-SH (black) and HS-P4-SH with 15 Å Al (dark gray), 30 Å Al (gray), and 30 Å Ti (gray). A vertical offset for Al deposition is introduced for clarity.

the chemical and structural stability of these SAMs. In this letter, we report grazing-incidence Fourier transform infrared (GI-FTIR) spectroscopy data of vapor-deposited metal overlayers of commonly used metals (Au, Al, and Ti) onto SAMs of conjugated, phenyl-based mono- and dithiols and a model system of hexadecanethiol ($C_{16}H_{33}$−SH). After thermal evaporation of the metals, the samples were transported through air (for several minutes) before the GI-FTIR analysis in nitrogen.

The detailed synthesis and characterization of phenyl-based mono- and dithiols and their SAMs were reported previously,[2] and the same assignments of the GI-FTIR active modes are used in this letter. These modes are compared to the GI-FTIR modes of oligophenylene mono- and -dithiol SAMs with vapor-deposited metal overlayers to determine changes on these SAMs caused by metal deposition. The chemical structures of the oligophenylene dithiols investigated are given in Figure 1 (HS-P_n-SH denotes the dithiol containing *n* phenyl rings). Figure 1 also shows infrared spectra of their SAMs before and after thermal or e-beam evaporation of 10 Å Au. As shown previously,[2] increasing the chain length from two to four phenyl rings gives rise to a more than linear increase of the aromatic C=C ring stretch intensity, indicating that the longer *p*-phenylene systems are oriented closer to the surface normal. Concerning Au deposition (Figure 1), we first note that we have no evidence of a substantial increase in broadband electronic absorption as might be expected for a percolated (continuous) metal overlayer,[24] indicating that only a small fraction of the outer surface is covered by Au. Deposition of 10 Å Au also leaves the position and intensity of the GI-FTIR modes unaffected. As the thickness of Au is increased, the intensity of the GI-FTIR indeed decreases (for 60 Å Au, a 50% decrease in intensity is observed) due to the screening effect of Au. But we did not observe any peak position change or new IR modes. Au thus neither causes chemical damage nor disturbs the conformation of the conjugated core of the dithiol SAM. In addition, there is no sign of broadening of the characteristic peaks, so the degree of order is unchanged. Such broadening would be related to the disturbance of the molecular packing and an indication of penetration of metal atoms into the monolayers.[16]

Therefore, penetration of Au into the SAM and insertion of Au in the thiol−gold bond at the gold substrate/organic interface (as reported for Au[12a,c] and Ag[9,11,12b] deposited on alkanethiols with a CH_3 end group at the organic/vacuum interface) is unlikely. Presumably, a noncontinuous gold layer (gold clusters) is deposited at the SAM/vacuum interface similar to gold deposited on octanedithiol.[12c,d] We conclude that the interaction between deposited Au and the thiol end groups at the SAM/vacuum interface reduces Au diffusion into the SAM[12c,d] and results in the formation of gold particles atop the SAM. Such interactions between deposited metal and OFGs are also found for aluminum deposited on hydroxy-terminated SAMs.[16] In this case, Al was found to be inserted into the O−H bond, forming O−Al−H. By contrast, for OCH_3-terminated SAMs, Al partially forms a metal overlayer and partially penetrates through the SAM to the SAM/Au substrate interface.[16]

To test the reactivity of thiol OFG toward Al, we have recorded GI-FTIR spectra of a SAM of HS-P4-SH before and after vapor deposition of 15 and 30 Å Al (15 Å, sample taken out for IR measurements followed by another 15 Å deposition) by thermal evaporation (Figure 2). Obviously, one can observe the growth of an aluminum oxide (Al_2O_3) layer, which is witnessed by a broad longitudinal-optical phonon mode around 900 cm^{-1} that increases with increasing aluminum exposure. All other observed modes assigned to HS-P4-SH[2] do not change significantly after Al deposition, except for some baseline fluctuations. This implies that Al deposition does not affect the conjugated backbone of oligophenylenedithiols. Al probably reacts with the −SH end groups and forms an aluminum overlayer. The Al layer then oxidizes upon air exposure during sample transfer from the growth chamber to the FTIR setup. Typically, a 2−3 nm thick Al_2O_3 layer can form spontaneously on Al. Unfortunately, the IR modes of the terminal C−S−H groups, and hence the interactions between Al and S−H of the SAM, could not be observed with GI-FTIR, since these modes are masked by the stronger aromatic ring stretch and bend modes. No significant broadening or shift of the IR peaks was observed. This implies that the conformations of the aromatic backbone are virtually undisturbed by the deposition of Al. The metal-induced spectral changes observed for HS-P4-SH are typical for Al deposition on all oligophenylenedithiols studied (HS-P2-SH and HS-P3-SH not shown). On all these SAMs, Al thus primarily interacts with the terminal thiol groups. Ti, on the other hand, completely destroys the HS-P4-SH SAM as is witnessed by the complete disappearance of the vibrational

(23) (a) Dhirani, A.; Lin, P.-H.; Guyot-Sionnest, P.; Zehner, R. W.; Sita, R. L. *J. Chem. Phys.* **1997**, *106*, 5249. (b) Metzger, R. M.; Xu, T.; Peterson, I. R. *J. Phys. Chem. B* **2001**, *105*, 1280. (c) Martin, A. S.; Sambles, J. R.; Ashwell, G. J. *Phys. Rev. Lett.* **1993**, *70*, 218.

(24) Fahsold, G.; Bartel, A.; Krauth, O.; Magg, N.; Pucci, A. *Phys. Rev. B* **2000**, *61*, 14108.

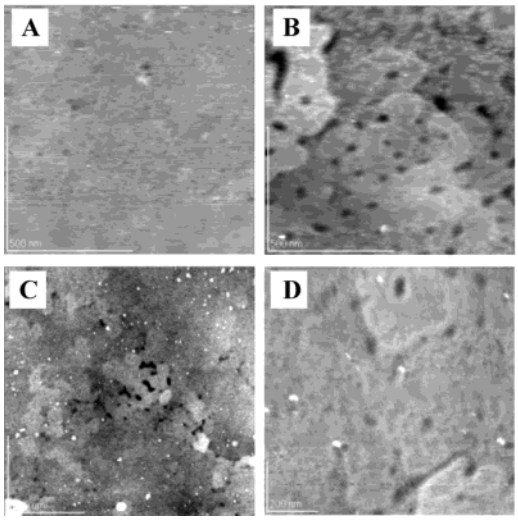

Figure 3. AFM images of HS-P4-SH before (panel A, 1 × 1 μm) and after deposition of 30 Å Au (panel B, 1 × 1 μm), Al (panel C, 3.3 × 3.3 μm), and Ti (panel D, 1 × 1 μm).

modes of HS-P4-SH. After the vapor deposition of 30 Å Ti, only a phonon mode of TiO_2 around 900 cm^{-1} is observed. The formation of carbides, oxycarbides, or a $Ti_wC_xO_yH_z$-like metastable film is expected.[14] Perhaps similar reactions also occur for Al to a certain degree, but not for Au.

Our infrared findings are supported by AFM data. We have recorded AFM images from over half a dozen dithiols when adsorbed as a pure monolayer, diluted (in a monothiol matrix), and with a variety of metal overlayers. When adsorbed as a dilute "impurity" in a mostly monothiol monolayer, some dithiols can be imaged with molecular resolution. When adsorbed pure, however, there is often significant tip−surface interaction. In some cases of pure dithiols, the images show a flat film with low roughness (<3 Å), while for other dithiols, it appears that there is intermittent transfer of material from the surface to the tip (and back). Passivation of the exposed thiol mitigates this effect. Simple air exposure for 1−2 days usually is sufficient to passivate by oxidizing the exposed thiol group.

AFM images for Au, Al, and Ti vapor-deposited onto a SAM of quaterphenyl dithiol (HS-P4-SH) on Au/mica substrates, which we have previously characterized by GI-FTIR,[2] are shown in Figure 3. For the Au case (Figure 3B), the most stable images were recorded after a 1−2 day passivation period. The 30 Å Au films were rough (~3 nm Au clusters) and showed preferential clustering near the step edges. For the Ti and Al cases, the films could be scanned immediately after metal adsorption. On the terraces they appear quite flat, with a much lower density of clustering.

Our interpretation is that the Al and Ti do react with the exposed thiol group, forming a relatively flat ultrathin overlayer. In the case of Al (Figure 3C), the average thickness of the reaction layer may be under 1 nm, with subsequent Al clustering on top of this layer. For the Ti (Figure 3D), based on the FTIR and AFM data, it appears that the Ti continues to react with the film (forming a complex Ti_xC_y) layer, until it is fully reacted. Once fully reacted, then the additional Ti can agglomerate into clusters.

In all cases, kinetics and thermodynamics (especially local bond strengths) will determine which channel the metal prefers (diffusion into the organic film, simple adsorption on the thiol end group, reactive adsorption with the organic backbone, or surface diffusion to form metal clusters). Although all three metals might be expected to bond with the thiol end group, the Au−S bond is weaker than the Au−Au bond, and during vacuum deposition, Au mobility is high enough that clustering on top of the dithiol is still a preferred channel (under our deposition conditions).

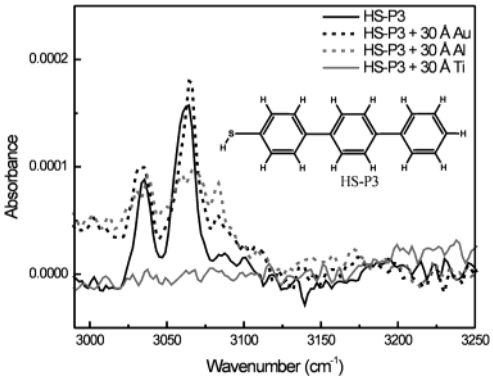

Figure 4. High-frequency region of the GI-FTIR spectra of HS-P3 before (black solid) and after deposition of 30 Å Au (black dotted), Al (gray dotted), and Ti (gray solid).

The importance of the type of end group at the organic/vacuum interface is demonstrated by depositing Au, Al, and Ti onto a SAM of a conjugated monothiol, namely, 4-monomercapto-*p*-terphenyl (HS-P3) as depicted in Figure 4. Since monothiols have no OFGs at the SAM/vacuum interface that can react with and block the incoming metal during vapor deposition, we expect metal atoms to penetrate more easily into the SAM and interact with the conjugated backbone of HS-P3. Figure 4 displays the high-frequency region (aromatic C−H stretch vibrations) of the GI-FTIR spectra of the HS-P3 SAM before and after metal deposition. Deposition of 30 Å Au shows that the inert Au atoms hardly interact with the SAM. The aromatic C−H stretch peaks exhibit the same intensity as for the bare HS-P3 SAM. In contrast to all metal/SAM systems discussed so far, the deposition of 30 Å Al onto the conjugated monothiol HS-P3 results in a strong decrease of C−H signal intensity due to strong interaction with the conjugated backbone. This confirms our expectation of metal penetration into the SAM. Ti destroys the SAM by reacting with the organic species, similar to the HS-P4-SH dithiol case discussed above: no aromatic C−H stretch vibrations were observed after the deposition of 30 Å Ti.

To explore whether the observed reactivity of SAMs toward Al and Ti is unique for aromatic rings, we tested a well-studied model substrate consisting of a hexadecanethiol ($C_{16}H_{33}$−SH) SAM. Hexadecanethiol is known to form a densely packed monolayer on Au(111) with a nearest neighbor spacing of ~0.5 nm in a $(\sqrt{3} \times \sqrt{3})$R30° superlattice. This SAM has been studied extensively with GI-FTIR[25] since its discovery. Figure 5 shows the high-frequency region of the GI-FTIR spectra of hexadecanethiol before and after metal deposition. The peak positions for a freshly prepared SAM are identical to those reported for a highly crystalline and trans-chain-conformation hexadecanethiol SAM.[25]

Deposition of Au and Al attenuates the Fermi resonances[26] (FR) of the terminal CH_3 stretch vibration at

(25) (a) Porter, M. D.; Bright, T. B.; Allara, D. L.; Chidsey, C. E. D. *J. Am. Chem. Soc.* **1987**, *109*, 3559. (b) Dubois, L. H.; Nuzzo, R. G. *Annu. Rev. Phys. Chem.* **1992**, *43*, 437.

(26) If a fundamental mode and an overtone or combination band of the same symmetry species have nearly the same energy, symmetry mixing can render a dipole-forbidden fundamental mode observable; this phenomenon is termed "Fermi resonance".

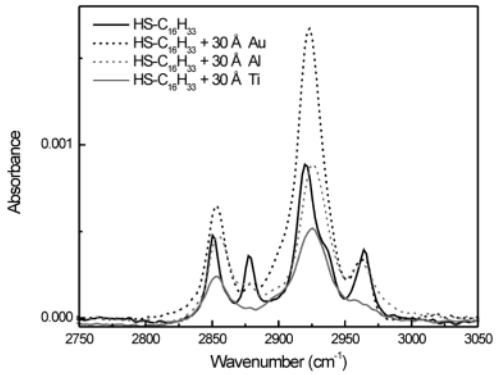

Figure 5. High-frequency region of the GI-FTIR spectra of hexadecanethiol before (black solid) and after deposition of 30 Å Au (black dotted), Al (gray dotted), and Ti (gray solid).

Table 1. Peak Positions for HS−$C_{16}H_{33}$ SAMs Adsorbed on Gold with and without Metal Overlayers

sample	ν_s CH_2 (cm^{-1})	ν_a CH_2 (cm^{-1})	ν_a (ip) CH_3 (cm^{-1})	ν_s CH_3 (FR) (cm^{-1})
HS−$C_{16}H_{33}$	2850	2919	2964	2877, 2937
HS−$C_{16}H_{33}$ + 30 Å Au	2853	2924	2962	2879
HS−$C_{16}H_{33}$ + 30 Å Al	2853	2925	2963	2877
HS−$C_{16}H_{33}$ + 30 Å Ti	2854	2926	*a*	*a*
crystalline[b]	2851	2918	*c*	*d*
liquid[b]	2855	2924	*c*	*d*

[a] Not observed. [b] Data taken from ref 25a. [c] ν_a (ip) masked by the strong ν_a (op) in the crystalline and liquid spectra. [d] Both ν_s (FR) bands are masked by the ν_a (CH_2) band.

2879 and 2937 cm^{-1}, indicating a strong interaction between Au/Al and the CH_3 terminus. Furthermore, a blue shift of the CH_2 asymmetric (ν_a) and symmetric (ν_s) stretching modes (Table 1) is observed, indicating a more liquidlike SAM. We attribute this to a decreased interchain interaction and the formation of a more disordered monolayer due to penetration of Au/Al atoms into the monolayer, which was not observed for the conjugated dithiols described above. The peak intensity of both CH_2 stretch modes is significantly stronger after Au deposition. This is most likely due to contaminants physisorbed on the Au overlayer during air exposure. In contrast to Au and Al, highly reactive Ti destroys[9,14] the hexadecanethiol SAM, similar to Ti deposition on the conjugated monothiol HS-P3.

In summary, Au, Al, and Ti overlayers were vapor-deposited onto SAMs of phenylene-based mono- and dithiols and hexadecanethiol and studied with GI-FTIR. Au and Al do not react with the conjugated backbone of the dithiols but, most likely, react with the thiol groups that are exposed at the SAM/vacuum interface. Only Ti completely destroys the conjugated dithiol SAMs. Also for monothiols, without a reactive OFG at the SAM/vacuum interface, the deposition of Au atoms occurs mainly at that interface, although penetration of inert Au atoms into the SAM and diffusion to the S−Au bond cannot be excluded. By contrast, vapor-deposited Al clearly interacts with the (conjugated) backbone of the monothiols. Ti completely destroys also the conjugated monothiol SAMs. The same order of reactivity (Au < Al < Ti) was found for methoxy-terminated alkanethiol SAMs in a previous study,[18] and the destruction of SAM by Ti appears to be a general phenomenon as well.[14,18]

Our study illustrates the importance of an understanding of metal−OFG interaction in designing and controlling metallic contacts for molecular electronics. Potential complications in metal vapor deposition onto SAMs include the penetration of metal atoms into SAMs lacking an appropriate OFG (and, consequently, the formation of shorts) and, most importantly, the destruction of the SAMs by highly reactive metals such as Ti, which is often used as an adhesion layer for gold top electrode in SAM-based molecular electronics. In light of our findings reported in this letter and others,[14,18] the interpretation of the properties of SAM-based electronic devices may need to be re-examined. In the choice of materials for future molecular electronic devices, it will be crucial to ensure appropriate reactivities of the electrode materials and the SAM functional end groups.

Acknowledgment. The authors thank their colleagues H. Meng, N. Zhitenev, D. Abusch-Magder, A. Erbe, H. E. Katz, J. Hsu, E. A. Chandross, and E. Reichmanis for helpful discussions. Support from The Netherlands Organization for Scientific Research (NWO, TALENT fellowship) to B.d.B. is gratefully acknowledged. M.M.F. was supported by a fellowship within the Postdoc Program of the German Academic Exchange Service (DAAD). E.G. and W.J. acknowledge the support of the New Jersey Center for Organic Opto-Electronics.

LA0356349